

## Enhanced Inactivation of *Bacillus subtilis* Spores during Solar Photolysis of Free Available Chlorine

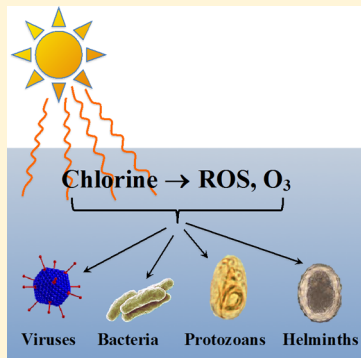
Jenna E. Forsyth,<sup>†</sup> Peiran Zhou,<sup>†</sup> Quanxin Mao,<sup>†</sup> Shelby S. Asato,<sup>†</sup> John S. Meschke,<sup>†,‡</sup> and Michael C. Dodd\*,<sup>†</sup>

<sup>†</sup>Department of Civil and Environmental Engineering, University of Washington, 201 More Hall, Box 352700, Seattle, Washington 98195, United States

<sup>‡</sup>Department of Environmental and Occupational Health Sciences, University of Washington, Box 357234, Seattle, Washington 98195, United States

### Supporting Information

**ABSTRACT:** Aqueous free available chlorine (FAC) can be photolyzed by sunlight and/or artificial UV light to generate various reactive oxygen species, including  $\text{HO}^\bullet$  and  $\text{O}^{(3)\text{P}}$ . The influence of this chemistry on inactivation of chlorine-resistant microorganisms was investigated using *Bacillus subtilis* endospores as model microbial agents and simulated and natural solar radiation as light sources. Irradiation of FAC solutions markedly enhanced inactivation of *B. subtilis* spores in 10 mM phosphate buffer; increasing inactivation rate constants by as much as 600%, shortening inactivation curve lag phase by up to 73% and lowering *CTs* required for  $2 \log_{10}$  inactivation by as much as 71% at pH 8.0 and 10 °C. Similar results were observed at pH 7.4 and 10 °C in two drinking water samples with respective DOC concentrations and alkalinities of 0.6 and 1.2 mg C/L and 81.8 and 17.1 mg/L as  $\text{CaCO}_3$ . Solar radiation alone did not inactivate *B. subtilis* spores under the conditions investigated. A variety of experimental data indicate that the observed enhancements in spore inactivation can be attributed to the concomitant attack of spores by  $\text{HO}^\bullet$  and  $\text{O}_3$ , the latter of which was found to accumulate to micromolar concentrations during simulated solar irradiation of 10 mM phosphate buffer (pH 8, 10 °C) containing  $[\text{FAC}]_0 = 8 \text{ mg/L}$  as  $\text{Cl}_2$ .



### INTRODUCTION

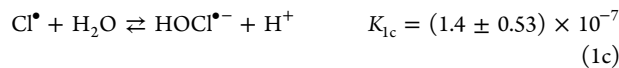
Aqueous free available chlorine (FAC)—primarily comprising  $\text{HOCl}$  ( $\text{pK}_a = 7.5$  at 25 °C<sup>1</sup>) and its conjugate base  $\text{OCl}^-$  at circumneutral pH—is inexpensive, easy to use, and one of the most common disinfectants applied in treatment of municipal drinking water and wastewater.<sup>2</sup> FAC is generally highly effective as a disinfectant, especially at lower pH, where the contribution of  $\text{HOCl}$  to disinfection reactions typically accelerates inactivation.<sup>3</sup> However, FAC is relatively ineffective against some important chlorine-resistant pathogenic agents such as *Giardia lamblia* cysts and *Cryptosporidium parvum* oocysts.<sup>4</sup> In addition, FAC treatment is well-known to result in the formation of various halogenated disinfection byproducts (DBPs).<sup>5</sup> As a consequence of these shortcomings, many utilities have transitioned from FAC as a primary disinfectant to UV, ozone ( $\text{O}_3$ ), or combined disinfectants, followed by FAC as a secondary disinfectant, with the aim of minimizing DBP formation while maintaining adequate levels of protection from microbial contamination.<sup>2,4</sup>

Substantial research conducted over the past decade has highlighted the possible benefits of combining two or more disinfectants, either in sequence or in parallel, to yield enhanced pathogen inactivation beyond that achievable by an individual disinfectant. For example, predisinfection with an oxidant capable of yielding substantial cell wall, oocyst wall, or spore coat damage (e.g.,  $\text{O}_3$  or  $\text{ClO}_2$ ), followed by postdisinfection with FAC, has been shown to substantially enhance the susceptibility

of microbial agents (including *C. parvum* oocysts) to inactivation in comparison to FAC alone.<sup>6–9</sup> A more recent study by Cho et al.<sup>10</sup> indicates that  $\text{HO}^\bullet$ , when utilized as a preoxidant, could also enhance sensitivity of some model microbial agents (including *Bacillus subtilis* spores and MS2 phage) to subsequent inactivation by FAC.

While these studies confirm that the sequential application of disinfectants can be advantageous, the process of combining disinfectants in practice can be operationally complex. It is therefore notable that FAC itself can serve as an *in situ* photochemical source of reactive oxygen species (ROS), including  $\text{HO}^\bullet$  and atomic oxygen ( $\text{O}^{(3)\text{P}}$ )—a precursor to  $\text{O}_3$ ,<sup>11,12</sup> allowing for the possible implementation of a single-step approach to disinfection that combines exposure to FAC and such oxidants *in situ*.

As shown in Table 1, homolytic cleavage of  $\text{HOCl}$  and  $\text{OCl}^-$  during exposure to light with  $\lambda < 400 \text{ nm}$  yields  $\text{HO}^\bullet$  or its conjugate base,  $\text{O}^{(3)\text{P}}^-$  ( $\text{pK}_a = 11.9 \pm 0.2$ <sup>13</sup>), and chlorine atom ( $\text{Cl}^\bullet$ ) (eqs 1a and 1b),<sup>12</sup> which may in turn react with water to yield additional  $\text{HO}^\bullet$  (eqs 1c<sup>14</sup> and 1d<sup>14</sup>).



Received: April 30, 2013

Revised: August 12, 2013

Accepted: August 15, 2013

Published: November 6, 2013

Table 1. Summary of Primary FAC Photolysis Pathways and Consequent ROS Formation

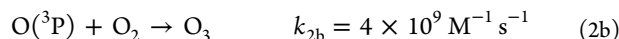
reaction		$\Phi(\lambda)$		
		254 nm	313 nm	365 nm
HO <sup>•</sup> formation:				
HOCl + $h\nu$ → HO <sup>•</sup> + Cl <sup>•</sup>	(1a)	0.46–1.4 <sup>17–19,a</sup>	1 <sup>20,b</sup>	ND <sup>d</sup>
OCl <sup>−</sup> + $h\nu$ → O <sup>•−</sup> + Cl <sup>•</sup>	(1b)	0.278 <sup>12</sup>	0.127 <sup>12</sup>	0.08 <sup>12</sup>
O( <sup>3</sup> P) formation: <sup>c</sup>				
OCl <sup>−</sup> + $h\nu$ → Cl <sup>−</sup> + O( <sup>3</sup> P)	(2a)	0.074 <sup>12</sup>	0.075 <sup>12</sup>	0.28 <sup>12</sup>
O( <sup>1</sup> D) formation:				
OCl <sup>−</sup> + $h\nu$ → Cl <sup>−</sup> + O( <sup>1</sup> D)	(3)	0.133 <sup>12</sup>	0.02 <sup>12</sup>	0 <sup>12</sup>

<sup>a</sup>The substantial variation in reported  $\Phi$  values for eq 1a at 254 nm has been attributed to variability in experimental conditions (e.g., different FAC concentrations, light sources, and HO<sup>•</sup> probe type).<sup>19</sup> <sup>b</sup>At approximately 310 nm in the gas phase. <sup>c</sup>Photolysis of HOCl is not known to generate O(<sup>3</sup>P).<sup>12,21,22</sup> <sup>d</sup>ND = Not determined.

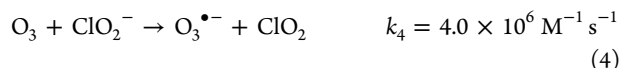


The homolytic pathway diminishes in importance with increasing wavelength of light (Table 1). In contrast, heterolytic cleavage of OCl<sup>−</sup> yields ground-state atomic oxygen (O(<sup>3</sup>P)) and chloride ion (Cl<sup>−</sup>), with increasing  $\Phi$  versus wavelength of light (Table 1, eq 2a).<sup>12</sup> At wavelengths below 320 nm, heterolytic FAC photolysis may also generate singlet-state atomic oxygen (O(<sup>1</sup>D)) (Table 1, eq 3). However, this species reacts rapidly with H<sub>2</sub>O ( $k = 1.8 (\pm 0.8) 10^{10} \text{ M}^{-1} \text{ s}^{-1}$ )<sup>68</sup> to yield H<sub>2</sub>O<sub>2</sub> and HO<sup>•</sup>.<sup>12,15</sup>

Under oxic conditions, O(<sup>3</sup>P) can react with O<sub>2</sub> in competition with OCl<sup>−</sup>, yielding the potent disinfectant O<sub>3</sub> in the former case (eq 2b<sup>16</sup>), and ClO<sub>2</sub><sup>−</sup> in the latter case (eq 2c<sup>12,16</sup>).



Subsequent reaction of O<sub>3</sub> with ClO<sub>2</sub><sup>−</sup> may then yield the additional disinfectant ClO<sub>2</sub> (eq 4<sup>23</sup>).



To date, FAC photolysis has been extensively investigated as an advanced oxidation process (AOP) for removing chemical contaminants from water.<sup>17–19,24–28</sup> However, it only appears to have been studied to a limited degree as an advanced disinfection process; primarily using 254 nm light as a source of photochemical activation.<sup>28</sup> Considering that the UV absorption spectra for OCl<sup>−</sup> and HOCl extend well above 300 nm (Supporting Information, Figure S1a), the use of sunlight or artificial UVA light for photochemical activation of FAC residuals would appear to represent an attractive means of augmenting traditional chlorination strategies for enhanced inactivation of chlorine-resistant pathogens. With this in mind, the present study focuses on the use of simulated and natural sunlight-driven FAC photolysis as a means of enhancing the inactivation of *B. subtilis* endospores, which were selected as model microbial agents on account of their high resistance to FAC,<sup>6,29</sup> and prior use as biological surrogates for disinfectant-resistant pathogenic microbial agents such as *C. parvum* oocysts.<sup>6,29–31</sup>

## MATERIALS AND METHODS

**Chemicals and Materials.** Commercially available chemicals were purchased from Sigma-Aldrich, with the exception of NaOCl—which was purchased from JT Baker—and Na<sub>2</sub>S<sub>2</sub>O<sub>3</sub>—

which was purchased from Fisher Scientific. All chemicals were of at least 95% purity, except for NaOCl, which was obtained as a ~5% available chlorine (w/v) solution, and NaClO<sub>2</sub>, which was obtained as a solid of 80% purity. FAC stock solutions were prepared by dilution of NaOCl, whereas O<sub>3</sub> and ClO<sub>2</sub> were generated immediately prior to use according to previously published procedures.<sup>32,33</sup> Working FAC, O<sub>3</sub>, and ClO<sub>2</sub> stock solutions were standardized spectrophotometrically at  $\lambda = 292$  nm, 258 nm, and 359 nm, using  $\epsilon_{292\text{nm},\text{OCl}^{\bullet-}} = 350 \text{ M}^{-1} \text{ cm}^{-1}$ <sup>34</sup>,  $\epsilon_{258\text{nm},\text{O}_3} = 3150 \text{ M}^{-1} \text{ cm}^{-1}$ ,<sup>35</sup> and  $\epsilon_{359\text{nm},\text{ClO}_2} = 1200 \text{ M}^{-1} \text{ cm}^{-1}$ ,<sup>36</sup> respectively. All solutions were prepared in Milli-Q water with resistivity  $\geq 18.2 \text{ M}\Omega \text{ cm}$ . Phosphate buffers and glassware were autoclaved at 121 °C for 15 min prior to use in order to ensure sterile conditions. Other reagents were sterilized by vacuum or syringe filtration using 0.22  $\mu\text{m}$  filters. Natural drinking water samples were obtained from two Seattle-area water treatment facilities and filter sterilized prior to use (Text S1, Table S1).

### Bacillus subtilis Spore Stock Preparation and Viability Assessment.

Endospores of *B. subtilis* strain ATCC 6633 were used as model microbial agents. Details of spore stock preparation can be found in Text S2. To the extent possible, a single spore stock (Stock 1) was used for experiments. Selected experiments undertaken with a second spore stock (Stock 2) are specifically noted. Spore viability was quantified by spot titering (Text S3).<sup>37</sup>

**Disinfection Procedures.** Experiments were generally undertaken in triplicate (unless otherwise noted), using natural water samples or 10 mM phosphate-buffered aqueous solutions at pH 6.0, 7.0, or 8.0, according to four basic approaches: (i) continuous irradiation of FAC solutions (“FAC + CL”, where CL = continuous light), (ii) brief irradiation of FAC solutions followed by cessation of irradiation and continued exposure to FAC in the dark (“FAC + BL”, where BL = brief light), (iii) exposure to FAC without irradiation (“FAC only”), or (iv) irradiation in the absence of FAC (“Light only”). Simulated sunlight experiments were undertaken at either 10 or 25 °C (maintained by means of a recirculating, constant temperature water bath), whereas natural sunlight experiments were undertaken without thermostating, at an ambient temperature of 33 °C. Maintenance of target temperatures in solution was confirmed by thermometer. Detailed descriptions of experimental procedures and reactor configurations can be found in Text S4.

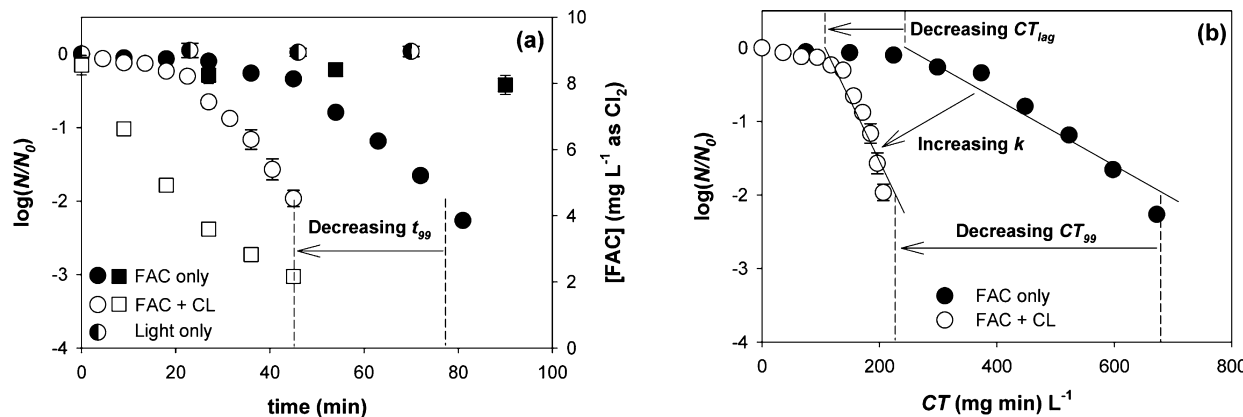


**Figure 1.** Influence of continuous simulated solar irradiation on enhancement of *B. subtilis* spore inactivation in 10 mM phosphate buffer (pH 8.0, 10 °C). (a) Spore viability (circles, left y-axis) and residual  $[FAC]$  (squares, right y-axis) versus time under FAC only, FAC + CL, and light only conditions. (b) FAC only and FAC + CL data plotted versus  $CT$ . See Table S2 (experiment 1) for additional experimental details.

## RESULTS AND DISCUSSION

### Analysis and Interpretation of Inactivation Data.

Inactivation of *B. subtilis* spores during exposure to FAC was characterized by a lag phase followed by a pseudo-first-order loss of spore viability (see Figure 1), consistent with the results of prior studies.<sup>6,29</sup> Such behavior can be described by a delayed Chick–Watson model, according to eq 5,<sup>38</sup>

$$\frac{N}{N_0} = \begin{cases} 1 & \text{if } CT \leq CT_{lag} = \frac{1}{k} \ln \left( \frac{N_1}{N_0} \right) \\ \exp(-k(CT - CT_{lag})) & \\ = \frac{N_1}{N_0} \exp(-kCT) & \text{if } CT > CT_{lag} = \frac{1}{k} \ln \left( \frac{N_1}{N_0} \right) \end{cases} \quad (5)$$

where  $CT$  is the integrated exposure to FAC over time (i.e.,  $\int_0^t [FAC] dt$ ) and  $N/N_0$  refers to the spore survival ratio (or residual viable spore concentration, in CFU/mL, normalized to initial viable concentration).  $\ln(N_1/N_0)$  and  $k$  refer to the magnitudes of the y-intercept and slope of a line fitted to the post-lag phase data points on a plot of  $\ln(N/N_0)$  versus  $CT$ , respectively, and  $CT_{lag}$  represents the extent of the lag phase—obtained from the x-intercept of the same fitted line. The relationships of these parameters to a generic plot of  $\ln(N/N_0)$  are illustrated in Figure S5.

The lag phase was operationally defined as comprising all data points in a plot of  $\ln(N/N_0)$  versus  $CT$  that deviated from the preceding point by less than two standard deviations about that point. The first data point to vary by at least two standard deviations from the preceding point was taken to mark the approximate end of the lag phase and beginning of pseudo-first-order decay. A least-squares linear fit through this and the subsequent data points was then used to more precisely determine  $k$  (in  $\text{L} (\text{mg min})^{-1}$ ) and  $CT_{lag}$  (in  $(\text{mg min}) \text{ L}^{-1}$ ). Values of  $CT_{99}$  (in  $(\text{mg min}) \text{ L}^{-1}$ ) and  $t_{99}$  (in minutes) were estimated using the equation of the fitted line and represent the  $CT$  and time, respectively, required to achieve 2  $\log_{10}$  units of spore inactivation.

Enhancements in inactivation resulting from irradiation are henceforth interpreted in terms of  $CT_{99}$  reduction factors (i.e., the ratio of  $CT_{99,0}/CT_{99}$ , with  $CT_{99,0}$  and  $CT_{99}$  representing values in the absence and presence of irradiation, respectively),  $CT_{lag}$  reduction factors ( $CT_{lag,0}/CT_{lag}$ ), and  $k$  enhancement

factors ( $k/k_0$ ), with inactivation data generally presented graphically in  $\log_{10}$  scale for convenience. Although the same spore stock (Stock 1) was utilized in all but a few experiments and uniform spore purification procedures were followed before each experiment, there was nevertheless some variability in spore response from one experiment to the other. Therefore, calculation of enhancement parameters for a given condition was performed using only results obtained from matched experiments conducted on the same day. Table S2 provides a summary of results obtained for the tested conditions.

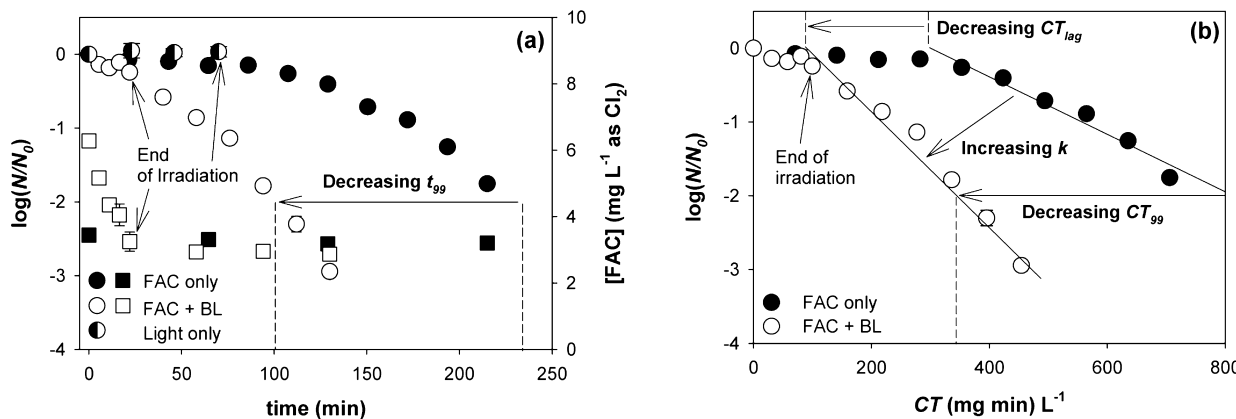
### Enhancement of Spore Inactivation during FAC Photolysis. Continuous Irradiation.

Figure 1 compares measurements of *B. subtilis* spore viability in 10 mM phosphate buffer (pH 8.0, 10 °C) during exposure to simulated sunlight alone (light only), FAC alone (FAC only), and FAC + continuous simulated sunlight (FAC + CL), where the same initial concentration of  $[FAC]_0 = 8.6 \text{ mg/L}$  as  $\text{Cl}_2$  was used in FAC only and FAC + CL experiments.

As shown in Figure 1a, exposure to FAC alone yielded gradual inactivation of spores at exposure times in excess of  $\sim 40$  min under these conditions. In contrast, exposure to light alone had no direct impact on spore viability over the irradiation time-scales utilized in these experiments (Figure 1a), or in any other experiments undertaken during this investigation (Figure S6). However, the combination of FAC and simulated sunlight (FAC + CL) led to a marked increase in the efficiency of spore inactivation, where spores exposed to the same level of  $[FAC]_0$  were inactivated nearly two times faster during irradiation than by FAC alone (i.e.,  $t_{99}$  values of 45 and 75 min were observed with and without irradiation, respectively).

Plotting the spore inactivation data in Figure 1a versus  $CT$  to account for variations in  $[FAC]$  reveals an even more pronounced effect of irradiation on inactivation efficiency than apparent from time-dependent plots (Figure 1b). Inactivation is clearly enhanced through a combination of lag phase reduction ( $CT_{lag,0}/CT_{lag} = 2.2$ ) and accelerated inactivation kinetics ( $k/k_0 = 4.0$ ), leading to an overall  $CT_{99}$  reduction factor of 3.0 for these conditions (Table S2). Taken together, these data strongly indicate a role of photochemically generated secondary oxidants in accelerating spore inactivation during FAC photolysis.

**Brief Irradiation.** Figure 2 depicts observed trends in spore viability during a similar series of experiments in which light only and FAC only controls were compared with FAC solutions



**Figure 2.** Influence of brief simulated solar irradiation on enhancement of *B. subtilis* spore inactivation in 10 mM phosphate buffer (pH 8.0, 10 °C). (a) Spore viability (circles, left y-axis) and residual [FAC] (squares, right y-axis) versus time under FAC only, FAC + BL, and light only conditions. (b) FAC only and FAC + BL data plotted versus CT. See Table S2 (experiment 2) for additional experimental details.

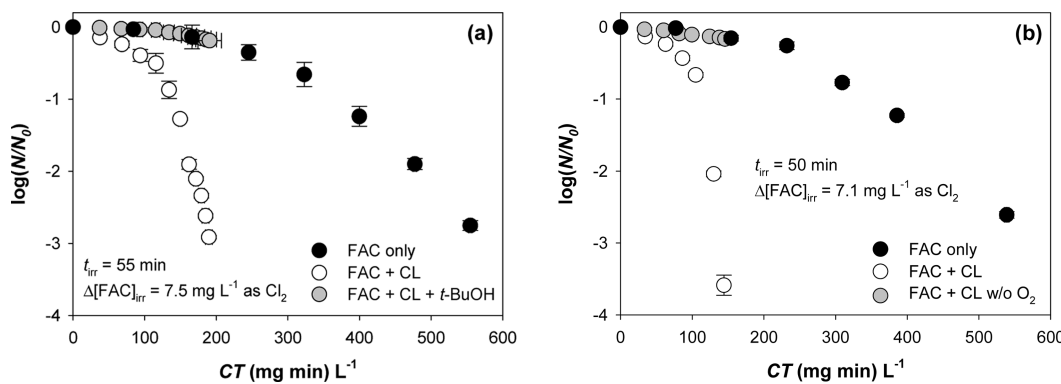


**Figure 3.** *B. subtilis* spore viability versus CT in 10 mM phosphate buffer (pH 8.0, 10 °C) in the presence and absence of (a) 50 mM *t*-BuOH, or (b)  $O_2$ , during continuous exposure to simulated sunlight. All experimental data shown here were obtained using spores diluted from Stock 2. *t*-BuOH experiments were undertaken in triplicate, whereas  $[O_2]$  variation experiments were undertaken in duplicate.  $[O_2] = 9 \text{ mg L}^{-1}$  under oxic conditions at ambient  $p_{O_2}$ .  $t_{irr}$  = irradiation time and  $\Delta[\text{FAC}]_{irr}$  = quantity of FAC photolyzed during irradiation. See Table S2 (experiments 3 and 4) for additional experimental details.

irradiated with simulated sunlight for only a brief interval of time (FAC + BL) rather than continuously. In this case, FAC only experiments were conducted using  $[\text{FAC}]_0 = 3.4 \text{ mg L}^{-1} \text{ as Cl}_2$ . FAC + BL experiments were conducted using an initial concentration of  $[\text{FAC}]_0 = 6.3 \text{ mg L}^{-1} \text{ as Cl}_2$  and irradiated for a time,  $t_{irr}$ , sufficient to photolyze  $\Delta[\text{FAC}]_{irr} = 3.0 \text{ mg L}^{-1} \text{ as Cl}_2$  (leaving a residual of  $3.3 \text{ mg L}^{-1} \text{ as Cl}_2$  in solution), after which the irradiated solutions were placed in the dark for continued monitoring of spore viability.

As shown in Figure 2b, the overall enhancement in inactivation efficiency achieved by brief irradiation—while not as large as observed during continuous irradiation—was nevertheless quite substantial ( $CT_{99,0}/CT_{99} = 2.3$ ; Table S2). It is also apparent from Figure 2b that spores exposed to a brief interval of solar irradiation and subsequently placed in the dark were inactivated significantly faster under dark conditions than spores in nonirradiated (i.e., FAC only) controls after normalizing for CT ( $k/k_0 = 1.8$ ; Table S2). This finding suggests that damage sustained by the spores during FAC photolysis sensitizes them to subsequent reaction with FAC even in the absence of light.

In contrast, no enhancement of spore inactivation was observed if spores were dosed to briefly preirradiated FAC solutions *after* removal of such solutions from simulated sunlight (Figure S7). This in turn suggests that enhancement results from sustained

*in situ* exposure of spores to low levels of secondary oxidants generated during FAC photolysis.

**Importance of Secondary Oxidants Generated during FAC Photolysis.** As noted in Table 1 and the accompanying discussion, FAC photolysis may yield a variety of reactive species that could be either directly or indirectly responsible for the trends in spore inactivation observed in Figures 1 and 2, including  $\text{HO}^\bullet$ ,  $\text{O}^{(3P)}$ ,  $\text{O}_3$ , and  $\text{ClO}_2$ . Of these species,  $\text{HO}^\bullet$ ,  $\text{O}_3$ , and  $\text{ClO}_2$  have each been reported to enhance the effectiveness of FAC as a disinfectant when using *B. subtilis* spores as model microorganisms.<sup>6,10,29</sup> To evaluate the likelihood that these latter three species contribute to acceleration of spore inactivation during FAC photolysis, a series of experiments was undertaken with the aim of quantifying their *in situ* concentrations in FAC solutions exposed to continuous simulated sunlight.

In order to quantify  $\text{HO}^\bullet$ , solutions of 10 mM phosphate buffer (pH 8, 10 °C) dosed with  $[\text{FAC}]_0 = 8 \text{ mg/L}$  as  $\text{Cl}_2$  were amended with  $1 \mu\text{M}$  of the  $\text{HO}^\bullet$  probe *para*-chlorobenzoic acid (pCBA),<sup>10,17</sup> and irradiated according to the same procedures used to generate the data shown in Figure 1. Measurements of pCBA loss were in turn used to estimate a maximal  $\text{HO}^\bullet$  exposure, or  $CT_{\text{HO}^\bullet}$  ( $= \int_0^t [\text{HO}^\bullet] dt$ ), of approximately  $5.0 \times 10^{-8} (\text{mg min}) \text{ L}^{-1}$  under such conditions (Text S6, Figure S9a). This level is apparently too low to yield direct inactivation of the spores utilized here, as no inactivation of Stock 2 spores was

observed at  $CT_{HO^{\cdot}}$  levels up to  $6.0 \times 10^{-8}$  (mg min) L<sup>-1</sup> during exposure to HO<sup>·</sup> generated via H<sub>2</sub>O<sub>2</sub> photolysis under simulated sunlight, consistent with prior findings by Mamane et al.<sup>69</sup> (Text S4, Figure S10a). However, other investigators have reported that similar  $CT_{HO^{\cdot}}$  levels (up to  $3.0 \times 10^{-8}$  (mg min) L<sup>-1</sup>) are sufficient to yield ~0.5-log enhancement of *B. subtilis* spore inactivation during post-treatment with FAC in pH 7 phosphate buffered saline at 20° C.<sup>10</sup>

In order to quantify O<sub>3</sub>, solutions of 10 mM phosphate buffer (pH 8, 10 °C) dosed with  $[FAC]_0 = 8$  mg/L as Cl<sub>2</sub> were exposed to continuous simulated sunlight for various predefined times and treated with a solution containing NH<sub>4</sub>Cl and cinnamic acid – which reacts rapidly and selectively with O<sub>3</sub> to yield benzaldehyde in 1:1 stoichiometry<sup>40</sup> – according to the procedures described in Text S6. Measurements of benzaldehyde confirmed the presence of O<sub>3</sub> concentrations up to ~1.8 μM in these solutions during irradiation (Figure S9b). The fact that O<sub>3</sub> did not accumulate to higher levels during FAC photolysis may be due to a combination of its direct reaction with OCl<sup>-</sup> ( $k = 1.20 (\pm 0.15) \times 10^2$  M<sup>-1</sup>s<sup>-1</sup>),<sup>41</sup> as well as radical chain reactions initiated by low levels of ClO<sub>2</sub><sup>-</sup> (eq 4) and/or ClO<sub>2</sub> ( $k = 1.37 (\pm 0.05) \times 10^3$  M<sup>-1</sup>s<sup>-1</sup>).<sup>23,36</sup> Measured benzaldehyde concentrations were in turn used to estimate an O<sub>3</sub> exposure, or  $CT_{O_3}$  ( $= \int_0^t [O_3] dt$ ), of approximately 3.0 (mg min) L<sup>-1</sup> under such conditions (Figure S9b). This  $CT_{O_3}$  level is apparently not high enough to yield direct inactivation of spores, as a  $CT_{lag,O_3}$  value of 4.3 ( $\pm 0.4$ ) (mg min) L<sup>-1</sup> was measured for direct exposure of Stock 2 spores to O<sub>3</sub> alone under the same conditions (Figure S10b). However, prior investigators have reported that pre-exposure of ATCC 6633 spores to  $CT_{O_3}$  levels below  $CT_{lag,O_3}$  can lead to reductions in  $CT_{lag,FAC}$  during post-treatment of the same spores with FAC, with progressively greater reductions in  $CT_{lag,FAC}$  (up to complete elimination of FAC lag phase) as  $CT_{O_3}$  is increased to  $CT_{lag,O_3}$  during the pre-treatment step.<sup>29</sup>

Additional experiments were undertaken with the aim of quantifying in situ ClO<sub>2</sub> concentrations during FAC photolysis. This was attempted according to the same general approach used for O<sub>3</sub> quantification, but with glycine and the dye 2,2'-Azino-bis(3-ethylbenzothiazoline-6-sulfonic acid) (ABTS) substituted for NH<sub>4</sub>Cl and cinnamic acid, respectively, as described in Text S6. ClO<sub>2</sub> could not be detected under the same conditions at which HO<sup>·</sup> and O<sub>3</sub> were measured. Taking into account a detection limit of ~0.1 μM for the ABTS method as utilized here

(Text S6), this suggests that in situ ClO<sub>2</sub> concentrations did not exceed 0.1 μM and that  $CT_{ClO_2}$  values could therefore not have exceeded ~0.3 (mg min) L<sup>-1</sup> over the 50 min irradiation periods typical of these experiments. This is far below levels necessary to achieve direct spore inactivation or likely to yield an enhancement of spore inactivation by FAC under these conditions (Figure S10c, ref 6).

On the basis of the above, it appears that both HO<sup>·</sup> and O<sub>3</sub> may play a role in accelerating spore inactivation during FAC photolysis. In order to further examine the importance of each oxidant, losses of spore viability were compared during photolysis of FAC in 10 mM phosphate buffer (pH 8, 10 °C) dosed with  $[FAC]_0 = 8$  mg/L as Cl<sub>2</sub> in the presence and absence of 50 mM t-BuOH – a widely employed scavenger of HO<sup>·</sup>.<sup>39</sup> As shown in Figure 3a, no discernible enhancement in spore inactivation was observed over the  $CT_{FAC}$  ranges investigated in solutions containing t-BuOH, despite the fact that  $t_{irr}$  (= 55 min) and  $\Delta[FAC]_{irr}$  (= 7.5 mg L<sup>-1</sup> as Cl<sub>2</sub>) were the same under each condition (Table S2, Figure S8a). pCBA measurements confirmed that the level of t-BuOH utilized here was sufficient to scavenge >95% of HO<sup>·</sup> under such conditions (data not shown), whereas benzaldehyde measurements indicated only a modest (~20–30%) decrease in O<sub>3</sub> exposure (Figure S9b). This is consistent with the relatively high aqueous-phase rate constant for reaction of t-BuOH with HO<sup>·</sup> ( $k = 6 \times 10^8$  M<sup>-1</sup>s<sup>-1</sup>),<sup>53</sup> compared to the much lower aqueous-phase rate constant anticipated for reaction of t-BuOH with O<sup>(3)P</sup> ( $k \sim 2.5 \times 10^6$  M<sup>-1</sup>s<sup>-1</sup>) on the basis of gas-phase O<sup>(3)P</sup> kinetics data.<sup>39</sup> These results indicate that in the absence of HO<sup>·</sup>, the levels of O<sub>3</sub> to which spores are exposed under the conditions depicted in Figure 3a are not sufficient on their own to account for the enhancements in spore inactivation observed during FAC photolysis. However, this does not exclude the possibility that enhancements in inactivation attributable to O<sub>3</sub> may have been observed at  $CT_{FAC}$  values beyond the ranges depicted in Figure 3a, which were inherently limited by depletion of FAC during photolysis.

A similar set of experiments was undertaken to examine the influence of HO<sup>·</sup> on spore inactivation in the absence of O<sub>3</sub>. In this case, losses of spore viability were compared during photolysis of FAC in 10 mM phosphate buffer (pH 8, 10 °C) dosed with  $[FAC]_0 = 8$  mg/L as Cl<sub>2</sub> at equilibrium with atmospheric O<sub>2</sub> and in otherwise identical solutions from which

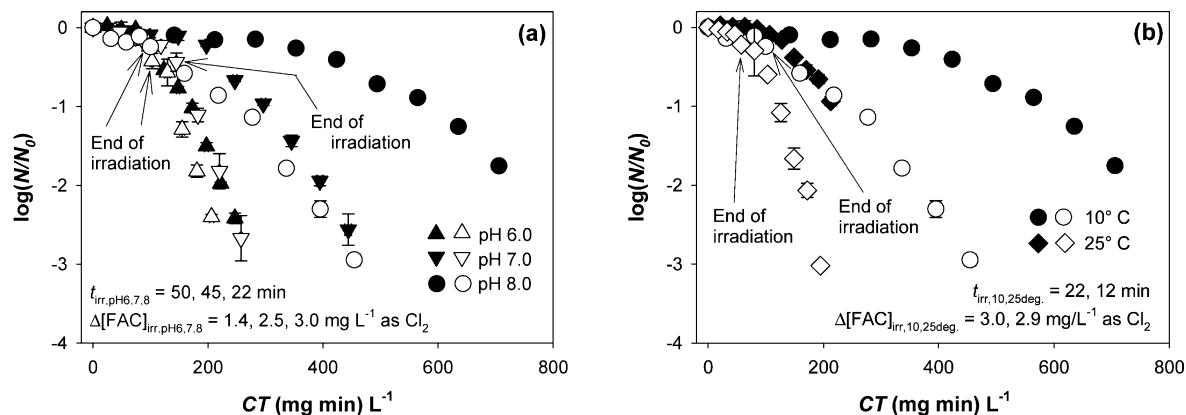


**Figure 4.** *B. subtilis* spore viability versus CT in 10 mM phosphate buffer with and without exposure to brief intervals of simulated sunlight (unfilled and filled symbols, respectively), at (a) pH 6.0, 7.0, and 8.0, all at 10 °C, and (b) pH 8.0 at 10 and 25 °C.  $t_{irr}$  = irradiation time and  $\Delta[FAC]_{irr}$  = quantity of FAC photolyzed during irradiation. See Table S2 (experiments 2 and 5–7) for additional experimental details. Note: The 25 °C data depicted here have been adapted with permission from ref 45.

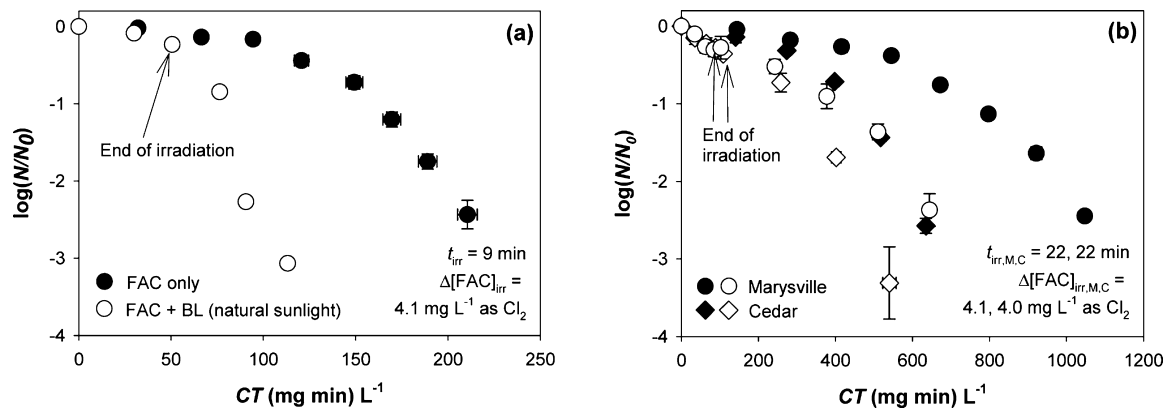


**Figure 5.** (a) *B. subtilis* spore viability versus  $CT$  in 10 mM phosphate buffer (pH 8.0, 33 °C) with and without brief exposure to natural sunlight (unfilled and filled symbols, respectively). Reactor configurations were as depicted in Figure S4d. (b) *B. subtilis* spore viability versus  $CT$  in natural water samples (pH 7.4, 10 °C) obtained from the Marysville and Cedar water treatment facilities, with and without brief exposure to simulated sunlight (unfilled and filled symbols, respectively).  $t_{\text{irr}}$  = irradiation time and  $\Delta[\text{FAC}]_{\text{irr}}$  = quantity of FAC photolyzed during irradiation. See Table S2 (experiments 8, 9, and 10) for additional experimental details.

$O_2$  had been removed by  $N_2$ -sparging (as a means of blocking  $O_3$  formation via eq 2b). As shown in Figure 3b, no enhancement of spore inactivation was observed in solutions lacking  $O_2$ , despite equal values of  $t_{\text{irr}}$  (= 50 min) and  $\Delta[\text{FAC}]_{\text{irr}}$  (= 7.1 mg L<sup>-1</sup> as  $Cl_2$ ) in the presence and absence of  $O_2$  (Table S2, Figure S8b). In analogy with the results obtained from the *t*-BuOH experiments (Figure 3a), this observation indicates that in the absence of  $O_3$ , the levels of  $HO^\bullet$  to which spores are exposed under the conditions depicted in Figure 3b are likewise insufficient on their own to account for the enhancements in spore inactivation observed during FAC photolysis. However, as noted for  $O_3$  in the context of the *t*-BuOH experiments, this does not exclude the possibility that enhancements in inactivation attributable to  $HO^\bullet$  alone may have been observed at  $CT_{\text{FAC}}$  values exceeding the ranges depicted in Figure 3b.

Taken together, the data presented in Figures 3a and 3b indicate that both  $HO^\bullet$  and  $O_3$  must be present during FAC photolysis to yield the observed enhancements in spore inactivation. This suggests that  $O_3$  and  $HO^\bullet$  likely play complementary roles, with one sensitizing spores toward inactivation by the other, and/or with both acting in concert to sensitize spores toward inactivation by FAC to a greater degree than achievable by either on its own.

Such effects would be consistent with prior findings by Cho and co-workers that simultaneous exposure to  $HO^\bullet$  can accelerate inactivation of *B. subtilis* ATCC 6633 spores during treatment with  $O_3$ ,<sup>29,42,43</sup> and that pre-exposure of spores to  $O_3 + H_2O_2$  can accelerate their inactivation by FAC to a greater extent than pre-treatment with comparable levels of  $O_3$  alone.<sup>43</sup> In line with these prior studies, it is hypothesized that  $O_3$  and  $HO^\bullet$  may elicit such enhancement effects during FAC photolysis by (a) accelerating the degradation of FAC-recalcitrant constituents of the protective spore coat, thereby sensitizing vital targets associated with the spore core to attack by FAC, as well as by (b) directly attacking vital targets once the spore coat is compromised. A more detailed discussion of the rationale for these hypotheses is presented in Text S7.

**Importance of pH, Temperature, Light Source, and Matrix Composition. Influence of pH.** Data from experiments conducted to examine the influence of pH on photolytic enhancement of spore inactivation—using the brief irradiation protocol described above—are summarized in Figure 4a. As shown here, values of  $k$  for spore inactivation in FAC only

solutions were inversely related to pH, consistent with a shift in FAC speciation from the more potent disinfectant HOCl toward  $OCl^-$  with increasing pH.<sup>4</sup> Similarly,  $CT_{\text{lag}}$  and  $CT_{99}$  under such conditions each increased by a factor of 3.5 with increasing pH from 6.0 to 8.0 (Table S2). These results are comparable to reports by other researchers of a ~4-fold variation in  $CT_{99}$  values for *B. subtilis* spores exposed to FAC between pH 5.6 and 8.2.<sup>6</sup>

It is also apparent from Figure 4a that the degree to which solar irradiation enhanced spore inactivation was actually significantly greater at higher pH, with  $CT_{99}$  reduction factors increasing from 1.2 to 2.3 between pH 6.0 and 8.0. This can likely be attributed to several factors. First, FAC photolysis kinetics are accelerated at higher pH, due to a shift in speciation toward  $OCl^-$ , which absorbs light much more effectively than HOCl (Figure S1a).<sup>44</sup> As a result, the quantity of FAC that can be photolyzed over a given  $t_{\text{irr}}$  increases as pH rises (as reflected in the  $\Delta[\text{FAC}]_{\text{irr}}$  values shown in Figure 4a). At the same time, an increase in pH should lead to higher  $O_3$  yields for a given  $\Delta[\text{FAC}]_{\text{irr}}$ , on account of the rise in  $O(^3P)$  production as FAC speciation shifts toward  $OCl^-$  (Table 1). Furthermore, because  $O_3$  does not exhibit acid–base speciation, its effectiveness as a disinfectant is less sensitive to changes in pH than for FAC.<sup>6,29,30</sup> Thus, the benefits of FAC photolysis become most apparent under conditions at which FAC itself is least effective.

**Influence of Temperature.** Figure 4b compares data from experiments conducted at 25 °C and pH 8.0 with those from the 10 °C, pH 8.0 experiments depicted in Figure 4a. As shown here,  $CT_{99}$  requirements decreased substantially in both irradiated and nonirradiated solutions as temperature was raised from 10 to 25 °C, consistent with the general positive influence of temperature on the effectiveness of FAC and  $O_3$  as disinfectants.<sup>4,31,46</sup> As a result,  $CT_{99,0}/CT_{99}$  remained essentially constant from 10 to 25 °C (Table S2). The degree of enhancement in spore inactivation thus appears to be relatively insensitive to temperature.

**Irradiation under Natural Sunlight.** To confirm that the results observed using simulated sunlight could be replicated with natural sunlight, a set of experiments was performed on the roof of the More Hall Civil and Environmental Engineering building at noon on a clear, spring day. The incident irradiance of direct natural sunlight during these experiments was determined to be a factor of 2.6 lower than that of the simulated sunlight source used in indoor experiments (Text S5). However, FAC

photolysis rates observed in outdoor experiments at pH 8 and 33 °C were actually a factor of 1.7 higher than in indoor experiments conducted at pH 8 and 25 °C (Figure S11). This is presumably due to a combination of higher temperature and the geometry of the quartz tubes used in outdoor experiments (Figure S4), which exposes solutions to light emanating from all directions and also results in increased internal reflectance of light.<sup>47,48</sup> Consequently, a relatively brief 9 min exposure to natural sunlight was sufficient to yield essentially the same reduction in  $CT_{99}$  requirements as observed for a 12 min exposure to simulated sunlight under these conditions, with  $CT_{99,0}/CT_{99} = 2.2$  in each case (Figure 5a, Table S2).

**Inactivation in Natural Water Samples.** Additional experiments were undertaken to assess the influence of natural water constituents on spore inactivation during FAC photolysis. The characteristics and sources of two natural water samples (Marysville and Cedar) utilized for this purpose are summarized in Text S1 and Table S1. As apparent from Figure 5b, spore inactivation in irradiated and nonirradiated samples was substantially slower for Marysville compared to Cedar. For example, the value of  $CT_{99}$  observed for FAC only experiments conducted in Marysville (979 (mg min) L<sup>-1</sup>) was almost twice that of  $CT_{99}$  in Cedar (575.4 (mg min) L<sup>-1</sup>), despite the waters having the same pH and Marysville actually having a lower DOC concentration than Cedar (Table S1). In fact, spore inactivation in the pH 7.4 Marysville sample was even slower than in pH 8 phosphate buffer (Table S2), despite the fact that FAC should have been more reactive at the lower pH of the natural water.

Because plotting inactivation data versus  $CT$  normalizes for variations in FAC concentration, and because similar effects were observed in the presence and absence of light, it is clear that the apparent recalcitrance of spores in Marysville cannot be due to differences in the rates at which FAC or secondary oxidants are consumed by matrix constituents. An alternative explanation for the increased spore resistance in Marysville may involve its higher concentrations of Mg<sup>2+</sup> and Ca<sup>2+</sup> compared to Cedar and pH 8 phosphate buffer. Ternary cell–cation–ligand complexes have been reported to form in solutions containing vegetative *B. subtilis* cells, various divalent cations, and DOM.<sup>49</sup> Additional investigations have shown that Ca<sup>2+</sup> is particularly effective at facilitating the attachment of DOM to MS2 bacteriophage and *C. parvum* oocyst surfaces,<sup>50,51</sup> as well as aggregation of individual viruses.<sup>52</sup> Presumably, similar interactions within the Marysville sample could have increased the resistance of *B. subtilis* spores to FAC, HO<sup>•</sup>, and/or O<sub>3</sub>.

Regardless, exposure to simulated sunlight led to appreciable enhancement of spore inactivation in both Marysville and Cedar, with a slightly greater  $CT_{99}$  reduction factor observed for Marysville (1.6) compared to Cedar (1.4). These values are somewhat lower than might be anticipated based on results observed for experiments undertaken in 10 mM phosphate buffer at pH 7.0 and 8.0 (for which respective  $CT_{99}$  reduction factors of 1.7 and 2.3 were observed at 10 °C). However, it is clear from these data that FAC photolysis has a beneficial effect on spore inactivation even in the presence of representative levels of alkalinity (which can scavenge ROS<sup>39,53</sup>) and DOM (which can scavenge ROS and O<sub>3</sub>,<sup>54,55</sup> as well as retard FAC photolysis via light screening<sup>44</sup>).

**Practical Considerations.** Before practical implementation of any approach utilizing FAC photolysis becomes feasible, it will be necessary to take into account the likely impacts of such processes on disinfection byproduct (DBP) formation in natural waters. For example, as noted above, O(<sup>3</sup>P) generated via

eq 2a can react with OCl<sup>−</sup> to yield ClO<sub>2</sub><sup>−</sup> (eq 2c). In addition, reactions of O(<sup>3</sup>P) with ClO<sub>2</sub><sup>−</sup> can lead to production of ClO<sub>3</sub><sup>−</sup> via eq 2d.<sup>12,16</sup>



Reactions of O<sub>3</sub> with OCl<sup>−</sup> and/or any ClO<sub>2</sub> generated via eq 4 may also serve as pathways to ClO<sub>3</sub><sup>−</sup> formation.<sup>23,36,41</sup> In Br<sup>−</sup>-containing waters, it is also possible that secondary reactions of HO<sup>•</sup> and O<sub>3</sub> with the HOBr/OB<sup>−</sup> generated upon reaction of Br<sup>−</sup> with FAC could contribute to BrO<sub>3</sub><sup>−</sup> formation.<sup>56</sup> As both ClO<sub>2</sub><sup>−</sup> and BrO<sub>3</sub><sup>−</sup> are currently regulated by the USEPA as DBPs, and ClO<sub>3</sub><sup>−</sup> is likely to be regulated in the near future, it is clear that development of strategies for minimizing their formation during FAC photolysis must be a particular focus of future research.

Future work will also require attention to factors influencing the formation of various organic DBPs, including regulated species such as trihalomethanes (THMs) and haloacetic acids (HAAs), and unregulated species such as nitrosamines, haloacetonitriles, halonitroalkanes, and cyanogen chloride. It has been reported that yields of chlorinated organics may be increased by irradiating FAC solutions with UVA or sunlight.<sup>57,58</sup> However, Oliver and Carey (1977) noted that chlorine incorporation was substantially diminished at higher pH, which they attributed to a shift from FAC homolysis (eqs 1a and 1b) to heterolysis (eq 2a), due to the dominance of OCl<sup>−</sup> above pH 7.5.<sup>58</sup> Furthermore, it remains unclear from prior studies whether FAC photolysis is more likely to lead to lower or higher DBP formation potential for a given  $CT$  level. Considering that yields of such DBP classes as THMs and HAAs are generally proportional to  $CT$  during chlorination processes<sup>59</sup> and that FAC photolysis may enable the use of lower  $CT$ s to achieve pathogen inactivation, it seems likely that implementation of FAC photolysis may actually enable appreciable *reductions* in formation of certain DBPs under appropriate conditions. For example, THM yields are generally understood to be higher at elevated pH.<sup>60–62</sup> Considering that FAC photolysis appears likely to yield the greatest reductions in  $CT$  requirements at higher pH (Figure 4a), it stands to reason that this process may be particularly well-suited to mitigating THM formation in mildly alkaline waters. This could potentially provide much the same benefit as practicing conventional chlorination with pH depression,<sup>59</sup> without the need for acidification of the treated water or the risk of enhanced HAA formation under acidic conditions.<sup>60–62</sup>

Provided that DBP formation during FAC photolysis can be properly managed, this approach could potentially offer a simple and relatively energy-efficient opportunity to improve inactivation of such chlorine-resistant waterborne pathogens as *C. parvum* oocysts, *G. lamblia* cysts, and *M. avium*, on account of their relative sensitivity to O<sub>3</sub>.<sup>4,63</sup> For example, the  $CT_{O_3}$  level of 3.0 (mg min) L<sup>-1</sup> determined from Figure S9b is in the range of values reported to achieve 0.5–1 log inactivation of *C. parvum* oocysts at  $T \geq 20$  °C<sup>38,64,65</sup> and is in significant excess of values necessary to achieve 3 log inactivation of *G. lamblia* cysts and various *M. avium* strains at typical ambient temperatures.<sup>46,63</sup>

Furthermore, the application of FAC photolysis processes could be technically feasible across a wide range of centralized and decentralized applications. For example, in a *centralized* setting, such as at a small municipal water treatment plant, FAC could be utilized in combination with UVA light-emitting diodes to achieve inactivation of chlorine-resistant microorganisms,

potentially at much lower operational energy costs than required for higher-energy germicidal UVC lamps. This could thereby simplify process configurations and operational maintenance requirements by combining irradiation and FAC exposure within a single application. Alternatively, in decentralized settings such as households in developing countries, FAC photolysis could be readily implemented by combining traditional solar water disinfection (SODIS) and chlorination—each of which is widely accessible in much of the world.<sup>66</sup> This could in turn provide a higher level of pathogen inactivation over shorter time-scales than achievable using either conventional chlorination or SODIS on its own<sup>67</sup> and—if practicing the brief irradiation setup described above—could also provide substantial protection against postdisinfection recontamination of treated water.

## ■ ASSOCIATED CONTENT

### Supporting Information

Texts, tables, and figures addressing natural water sample characteristics, spore stock preparation and viability assay, chemical analytical methods, disinfection procedures, spectroradiometry, experimental reactor configurations, and experimental conditions and results. This material is available free of charge via the Internet at <http://pubs.acs.org>.

## ■ AUTHOR INFORMATION

### Corresponding Author

\*Address: 305 More Hall, Box 352700; Seattle, WA 98195-2700. Phone: 206-685-7583; fax: 206-543-1543; e-mail: doddm@uw.edu.

### Notes

The authors declare no competing financial interest.

## ■ ACKNOWLEDGMENTS

J.E.F. gratefully acknowledges financial support from a U.S. National Science Foundation Graduate Research Fellowship (DGE-0718124). This work was also supported in part by U.S. National Science Foundation grant CBET-1236303. The authors thank Nicola K. Beck, José Méndez-Díaz, Douglas E. Latch, and Gwy-Am Shin for technical assistance and informative discussions. Alex Chen and Brad Zahnow are acknowledged for assistance in obtaining water samples from the Cedar and Marysville water treatment facilities, respectively. Four anonymous reviewers are thanked for their insightful comments and suggestions for strengthening this work.

## ■ REFERENCES

- (1) Morris, J. C. Acid ionization constant of HOCl from 5 to 35°. *J. Phys. Chem.* **1966**, *70*, 3798–3805.
- (2) *Community Water System Survey. Vol. II: Detailed Tables and Survey Methodology*; United States Environmental Protection Agency: Washington, DC, 2000.
- (3) Fair, G. M.; Morris, J. C.; Chang, S. L.; Weil, I.; Burden, R. P. The Behavior of Chlorine as a Water Disinfectant. *J. Am. Water Works Assoc.* **1948**, 1051–1061.
- (4) *Alternative Disinfectants and Oxidants Guidance Manual*; United States Environmental Protection Agency: Washington, DC, 1999.
- (5) Richardson, S. D. Disinfection by-products and other emerging contaminants in drinking water. *Trends Anal. Chem.* **2003**, *22*, 666–684.
- (6) Cho, M.; Kim, J. H.; Yoon, J. Investigating synergism during sequential inactivation of *Bacillus subtilis* spores with several disinfectants. *Water Res.* **2006**, *40*, 2911–2920.
- (7) Corona-Vasquez, B.; Samuelson, A.; Rennecker, J. L.; Marinas, B. J. Inactivation of *Cryptosporidium parvum* oocysts with ozone and free chlorine. *Water Res.* **2002**, *36*, 4053–4063.
- (8) Rennecker, J. L.; Driedger, A. M.; Rubin, S. A.; Marinas, B. J. Synergy in sequential inactivation of *Cryptosporidium parvum* with ozone/free chlorine and ozone/monochloramine. *Water Res.* **2000**, *34*, 4121–4130.
- (9) Rennecker, J. L.; Kim, J. H.; Corona-Vasquez, B.; Marinas, B. J. Role of disinfectant concentration and pH in the inactivation kinetics of *Cryptosporidium parvum* oocysts with ozone and monochloramine. *Environ. Sci. Technol.* **2001**, *35*, 2752–2757.
- (10) Cho, M.; Gandhi, V.; Hwang, T. M.; Lee, S.; Kim, J. H. Investigating synergism during sequential inactivation of MS-2 phage and *Bacillus subtilis* spores with UV/H<sub>2</sub>O<sub>2</sub> followed by free chlorine. *Water Res.* **2011**, *45*, 1063–1070.
- (11) Nowell, L. H.; Hoigne, J. Photolysis of aqueous chlorine at sunlight and ultraviolet wavelengths - 2. Hydroxyl radical production. *Water Res.* **1992**, *26*, 599–605.
- (12) Buxton, G. V.; Subhani, M. S. Radiation-chemistry and photochemistry of oxychlorine ions. 2. Photodecomposition of aqueous-solutions of hypochlorite ions. *J. Chem. Soc., Faraday Trans. 1* **1972**, *68*, 958–969.
- (13) Rabani, J.; Matheson, M. S. Pulse radiolytic determination of pK for hydroxyl ionic dissociation in water. *J. Am. Chem. Soc.* **1964**, *86*, 3175–3176.
- (14) Yu, X. Y. Critical evaluation of rate constants and equilibrium constants of hydrogen peroxide photolysis in acidic aqueous solutions containing chloride ions. *J. Phys. Chem. Ref. Data* **2004**, *33*, 747–763.
- (15) McGrath, W. D.; McGarvey, J. J. Production, deactivation and chemical reactions of O(<sup>1</sup>D) atoms. *Planet. Space Sci.* **1967**, *15*, 427–455.
- (16) Klaening, U. K.; Sehested, K.; Wolff, T. Ozone formation in laser flash photolysis of oxoacids and oxoanions of chlorine and bromine. *J. Chem. Soc., Faraday Trans. 1* **1984**, *80*, 2969–2979.
- (17) Watts, M. J.; Linden, K. G. Chlorine photolysis and subsequent OH radical production during UV treatment of chlorinated water. *Water Res.* **2007**, *41*, 2871–2878.
- (18) Jin, J.; El-Din, M. G.; Bolton, J. R. Assessment of the UV/chlorine process as an advanced oxidation process. *Water Res.* **2011**, *45*, 1890–1896.
- (19) Wang, D.; Bolton, J. R.; Hofmann, R. Medium pressure UV combined with chlorine advanced oxidation for trichloroethylene destruction in a model water. *Water Res.* **2012**, *46*, 4677–4686.
- (20) Molina, M. J.; Ishiwata, T.; Molina, L. T. Production of OH radical from photolysis of HOCl at 307–309 nm. *J. Phys. Chem.* **1980**, *84*, 821–826.
- (21) Butler, P. J. D.; Phillips, L. F. Upper limit for the atomic oxygen yield in the 308-nm photolysis of HOCl. *J. Phys. Chem.* **1983**, *87*, 183–184.
- (22) Vogt, R.; Schindler, R. N. Product channels in the photolysis of HOCl. *J. Photochem. Photobiol. A, Chem.* **1992**, *66*, 133–140.
- (23) Klaening, U. K.; Sehested, K.; Holcman, J. Standard Gibbs energy of formation of the hydroxyl radical in aqueous solution. Rate constants for the reaction ClO<sub>2</sub><sup>–</sup> + O<sub>3</sub> ↔ O<sub>3</sub><sup>–</sup> + ClO<sub>2</sub>. *J. Phys. Chem.* **1985**, *89*, 760–763.
- (24) Chan, P. Y.; El-Din, M. G.; Bolton, J. R. A solar-driven UV/Chlorine advanced oxidation process. *Water Res.* **2012**, *46*, 5672–5682.
- (25) Feng, Y.; Smith, D. W.; Bolton, J. R. Photolysis of aqueous free chlorine species (HOCl and OCl<sup>–</sup>) with 254 nm ultraviolet light. *J. Environ. Eng. Sci.* **2007**, *6*, 277–284.
- (26) Feng, Y.; Smith, D. W.; Bolton, J. R. A Potential New Method for Determination of the Fluence (UV Dose) Delivered in UV Reactors Involving the Photodegradation of Free Chlorine. *Water Environ. Res.* **2010**, *82*, 328–334.
- (27) Boal, A. K.; Pisarenko, A.; Olsen, B. E.; Stanford, B. D.; Snyder, S. A.; Rivera, S. B. Aqueous Chlorine Based Advanced Oxidative Processes: Research and Reuse Applications. Extended abstracts of the *International Congress on Sustainability Science & Engineering (ICOSSE)*, University of Arizona, Tucson, AZ, 2011.
- (28) Boal, A. K.; Olson, B. E.; Bajszar, G.; Snyder, S. A.; Stanford, B. D.; Rivera, S. B. Synergistic inactivation of *Bacillus globigii* spores using

combined aqueous chlorine and ultraviolet light. *Abstr. Pap. Am. Chem. Soc.* **2011**, 242.

(29) Cho, M.; Chung, H.; Yoon, J. Quantitative evaluation of the synergistic sequential inactivation of *Bacillus subtilis* spores with ozone followed by chlorine. *Environ. Sci. Technol.* **2003**, 37, 2134–2138.

(30) Larson, M. A.; Marinas, B. J. Inactivation of *Bacillus subtilis* spores with ozone and monochloramine. *Water Res.* **2003**, 37, 833–844.

(31) Driedger, A.; Staub, E.; Pinkernell, U.; Marinas, B.; Koster, W.; Von Gunten, U. Inactivation of *Bacillus subtilis* spores and formation of bromate during ozonation. *Water Res.* **2001**, 35, 2950–2960.

(32) Huber, M. M.; Korhonen, S.; Ternes, T. A.; von Gunten, U. Oxidation of pharmaceuticals during water treatment with chlorine dioxide. *Water Res.* **2005**, 39, 3607–3617.

(33) Bader, H.; Hoigné, J. Determination of ozone in water by the indigo method. *Water Res.* **1981**, 15, 449–456.

(34) Kumar, K.; Day, R. A.; Margerum, D. W. Atom-transfer redox kinetics: General-acid-assisted oxidation of iodide by chloramines and hypochlorite. *Inorg. Chem.* **1986**, 25, 4344–4350.

(35) Hoigné, J. In *The Handbook of Environmental Chemistry*; Hrubec, J., Ed.; Springer Verlag: Berlin, Germany, 1998; pp 83–141.

(36) Hoigne, J.; Bader, H. Kinetics of reactions of chlorine dioxide (OCIO) in water. 1. Rate constants for inorganic and organic compounds. *Water Res.* **1994**, 28, 45–55.

(37) Beck, N. K.; Callahan, K.; Nappier, S. P.; Kim, H.; Sobsey, M. D.; Meschke, J. S. Development of a spot-titer culture assay for quantifying bacteria and viral indicators. *J. Rapid Methods Autom. Microbiol.* **2009**, 17, 455–464.

(38) Rennecker, J. L.; Marinas, B. J.; Owens, J. H.; Rice, E. W. Inactivation of *Cryptosporidium parvum* oocysts with ozone. *Water Res.* **1999**, 31, 2481–2488.

(39) Reisz, E.; Schmidt, W.; Schuchmann, H.-P.; von Sonntag, C. Photolysis of ozone in aqueous solutions in the presence of tertiary butanol. *Environ. Sci. Technol.* **2003**, 37, 1941–1948.

(40) Leitzke, A.; Reisz, E.; Flyunt, R.; von Sonntag, C. The reactions of ozone with cinnamic acids: formation and decay of 2-hydroperoxy-2-hydroxyacetic acid. *J. Chem. Soc., Perkin Trans. 2* **2001**, 793–797.

(41) Haag, W. R.; Hoigne, J. Ozonation of water containing chlorine or chloramines. Reaction products and kinetics. *Water Res.* **1983**, 17, 1397–1402.

(42) Cho, M.; Chung, H. M.; Yoon, J. Disinfection of water containing natural organic matter by using ozone-initiated radical reactions. *Appl. Environ. Microbiol.* **2003**, 69, 2284–2291.

(43) Cho, M.; Yoon, J. Enhanced bactericidal effect of O<sub>3</sub>/H<sub>2</sub>O<sub>2</sub> followed by Cl<sub>2</sub>. *Ozone-Sci. Eng.* **2006**, 28, 335–340.

(44) Nowell, L. H.; Hoigne, J. Photolysis of aqueous chlorine at sunlight and ultraviolet wavelengths - 1. Degradation rates. *Water Res.* **1992**, 26, 593–598.

(45) Forsyth, J. E.; Mao, Q.; Meschke, J. S.; Dodd, M. C. Photochemical Activation of Free Chlorine to Reactive Oxygen Species for Enhanced Inactivation of Chlorine-Resistant Microorganisms. *Extended abstracts of the Water Environment Federation Disinfection and Public Health 2013*, Indianapolis, IN, 2013; Water Environment Federation.

(46) *Disinfection Profiling and Benchmarking Guidance Manual*; United States Environmental Protection Agency: Washington, DC, 1999.

(47) Dulin, D.; Mill, T. Development and evaluation of sunlight actinometers. *Environ. Sci. Technol.* **1982**, 16, 815–820.

(48) Haag, W. R.; Hoigne, J. Singlet oxygen in surface waters. 3. Photochemical formation and steady-state concentrations in various types of waters. *Environ. Sci. Technol.* **1986**, 20, 341–348.

(49) Borrok, D.; Aumend, K.; Fein, J. B. Significance of ternary bacteria-metal-natural organic matter complexes determined through experimentation and chemical equilibrium modeling. *Chem. Geol.* **2007**, 238, 44–62.

(50) Pham, M.; Mintz, E. A.; Nguyen, T. H. Deposition kinetics of bacteriophage MS2 to natural organic matter: Role of divalent cations. *J. Colloid Interface Sci.* **2009**, 338, 1–9.

(51) Janjaroen, D.; Liu, Y.; Kuhlenschmidt, M. S.; Kuhlenschmidt, T. B.; Nguyen, T. H. Role of divalent cations on deposition of *Cryptosporidium parvum* oocysts on natural organic matter surfaces. *Environ. Sci. Technol.* **2010**, 44, 4519–4524.

(52) Gutierrez, L.; Mylon, S. E.; Ferri, J.; Nash, B.; Nguyen, T. H. Deposition and aggregation kinetics of rotavirus in divalent cation solutions. *Environ. Sci. Technol.* **2010**, 44, 4552–4557.

(53) Buxton, G. V.; Greenstock, W. P.; Helman, W. P.; Ross, A. B. Critical review of rate constants for reactions of hydrated electrons, hydrogen atoms, and hydroxyl radicals (•OH/O•<sup>+</sup>) in aqueous solution. *J. Phys. Chem. Ref. Data* **1988**, 17, 513–886.

(54) Westerhoff, P.; Mezyk, S. P.; Cooper, W. J.; Minakata, D. Electron pulse radiolysis determination of hydroxyl radical rate constants with Suwannee river fulvic acid and other dissolved organic matter isolates. *Environ. Sci. Technol.* **2007**, 41, 4640–4646.

(55) von Gunten, U. Ozonation of drinking water: Part I. Oxidation kinetics and product formation. *Water Res.* **2003**, 37, 1443–1467.

(56) von Gunten, U. Ozonation of drinking water: Part II. Disinfection and by-product formation in presence of bromide, iodide, or chloride. *Water Res.* **2003**, 37, 1469–1487.

(57) Pisarenko, A. N.; Stanford, B. D.; Snyder, S. A.; Rivera, S. B.; Boal, A. K. Investigation of the use of Chlorine Based Advanced Oxidation in Surface Water: Oxidation of Natural Organic Matter and Formation of Disinfection Byproducts. *J. Adv. Oxid. Technol.* **2013**, 16, 137–150.

(58) Oliver, B. G.; Carey, J. H. Photochemical production of chlorinated organics in aqueous solutions containing chlorine. *Environ. Sci. Technol.* **1977**, 11, 893–895.

(59) Crittenden, J. C.; Trussell, R. R.; Hand, D. W.; Howe, K. J.; Tchobanoglous, G. *Water Treatment - Principles and Design*, 2nd ed.; John Wiley & Sons: Hoboken, NJ, 2005.

(60) Miller, J. W.; Uden, P. C. Characterization of non-volatile aqueous chlorination products of humic substances. *Environ. Sci. Technol.* **1983**, 17, 150–157.

(61) Reckhow, D. A.; Singer, P. C.; Malcolm, R. L. Chlorination of humic materials: Byproduct formation and chemical interpretations. *Environ. Sci. Technol.* **1990**, 24, 1655–1664.

(62) Obolensky, A.; Singer, P. C. Development and interpretation of disinfection byproduct formation models using the Information Collection Rule database. *Environ. Sci. Technol.* **2008**, 42, 5654–5660.

(63) Taylor, R. H.; Falkingham, J. O.; Norton, C. D.; LeChevallier, M. W. Chlorine, chloramine, chlorine dioxide, and ozone susceptibility of *Mycobacterium avium*. *Appl. Environ. Microbiol.* **2000**, 66, 1702–1705.

(64) *Long Term 2 Enhanced Surface Water Treatment Rule Toolbox Guidance Manual*; United States Environmental Protection Agency: Washington, DC, 2010.

(65) Li, H.; Gyurek, L. L.; Finch, G. R.; Smith, D. W.; Belosevic, M. Effect of temperature on ozone inactivation of *Cryptosporidium parvum* in oxidant demand-free phosphate buffer. *J. Environ. Eng.* **2001**, 127, 456–467.

(66) The Safe Water System (<http://www.cdc.gov/safewater/index.html>). Centers for Disease Control and Prevention, 2013.

(67) Fisher, M. B.; Keenan, C. R.; Nelson, K. L.; Voelker, B. M. Speeding up solar disinfection (SODIS): effects of hydrogen peroxide, temperature, pH, and copper plus ascorbate on the photoinactivation of *E. coli*. *J. Water Health* **2008**, 6, 35–51.

(68) Biedenkapp, D.; Hartshorn, L. G.; Bair, E. J. The O(<sup>1</sup>D) + H<sub>2</sub>O reaction. *Chem. Phys. Lett.* **1970**, 5, 379–380.

(69) Mamane, H.; Shemer, H.; Linden, K. G. Inactivation of *E. coli*, *B. subtilis* spores, and MS2, T4, and T7 phage using UV/H<sub>2</sub>O<sub>2</sub> advanced oxidation. *J. Hazard. Mater.* **2007**, 146, 479–486.